

Article

The Distribution of Gas Components within a Shale System and Its Implication for Migration

Bojiang Fan ^{1,2,3,*}, Liang Shi ³, Xia Wang ³, Chi Wang ³, Yating Li ³ and Feifei Huang ³

¹ State Key Laboratory of Shale Oil and Gas Enrichment Mechanisms and Effective Development, Beijing 102206, China

² Sinopec Key Laboratory of Shale Oil/Gas Exploration and Production Technology, Beijing 102206, China

³ School of Petroleum Engineering and Environmental Engineering, Yan An University, Yan'an 716000, China; yananshi2088@126.com (L.S.); oukawang@yau.edu.cn (X.W.); wc19829762673@163.com (C.W.); lytsummer@126.com (Y.L.); feifeihuang_upc@hotmail.com (F.H.)

* Correspondence: fanbj9@163.com; Tel.: +86-13571108754

Abstract: Experimental studies on the desorption and adsorption of shale are conducted extensively and used for in-depth research on shale gas components and isotopic components. However, there is little systematic research aimed at a given shale stratum. This study takes the Chang-7 shale of the YC23 Well in the Ordos Basin as the research object, and attempts to obtain a full understanding of the distribution characteristics of different gas components, and to explore the migration ability of different gas components. In this study, Chang-7 shale gas in Well YC23 can be sorted into three categories: generated gas, retained gas and accumulated gas. Geochemical parameters including TOC, S₁ and S₂ are used to evaluate the generated gas, and the fractionation of hydrocarbon components is used to distinguish retained gas and migrated gas. The fractionation of non-hydrocarbon components as well as carbon isotopes is also analyzed and discussed. This study confirms that shale gas in different locations has unique gas components due to gas migration.

Keywords: shale system; shale gas; desorption experiment; gas migration



Citation: Fan, B.; Shi, L.; Wang, X.; Wang, C.; Li, Y.; Huang, F. The Distribution of Gas Components within a Shale System and Its Implication for Migration. *Minerals* **2022**, *12*, 397. <https://doi.org/10.3390/min12040397>

Academic Editors: Rui Yang, Zhiye Gao, Yuguang Hou, Songtao Wu and Thomas Gentzis

Received: 15 February 2022

Accepted: 22 March 2022

Published: 24 March 2022

Publisher's Note: MDPI stays neutral with regard to jurisdictional claims in published maps and institutional affiliations.



Copyright: © 2022 by the authors. Licensee MDPI, Basel, Switzerland. This article is an open access article distributed under the terms and conditions of the Creative Commons Attribution (CC BY) license (<https://creativecommons.org/licenses/by/4.0/>).

1. Introduction

The successful development of shale gas has led to a better understanding of the adsorption of gas in shale by geologists. In some shale gas-producing areas, the high content of adsorbed gas has ensured the stable production of shale gas; indeed, some wells have been producing shale gas for more than 30 years. Thus, desorption experiments and adsorption experiments on shale are used extensively for in-depth research on shale gas components and isotopic components. Progress in the research on shale gas has been achieved by using the gas composition and isotopic composition as follows: (1) to evaluate the shale gas content—the methods for calculating lost gas are established, including calculating lost gas by combining the test results and gas diffusion theory, the United States Bureau of Mines (USBM) method and the polygonal curve fitting method [1–4]; (2) to explore the origins of shale gas—the origins of shale gas include biogenesis, thermogenesis, high-temperature pyrolysis, and mixed origins [4,5]; (3) to explore the migration ability of different gas components—due to the differences in the adsorption of mineral particles and kerogen and the dissolving of oil and water, hydrocarbon gases and non-hydrocarbon gases in the shale system show wide variations in migration ability [6–10]; (4) to explore the state of shale gas—the three gas states including the adsorbed state, free state and dissolved state have been studied and the corresponding calculation models are established [6,7,11,12]; and (5) to explore the evolutionary characteristics of shale gas in the geological periods—based on the geological conditions such as temperature and pressure, a dynamic simulation is carried out to assess the gas content and gas state [7,8,13].

Although studies focused on the migration ability of gas components have been done in recent years, there are few systematic studies aimed at a given shale stratum. In fact, the lacustrine shale system has strong heterogeneity, and it is easy to differentiate the shale gas components. A large number of studies have confirmed that sandy laminae and thin sandstone are highly developed within shale systems, and there is extensive organic heterogeneity (organic abundance, organic type, etc.) and reservoir heterogeneity (organic pore, inorganic pore, pore size, porosity and permeability) [14–20]. Taking the Chang-7 shale (Chang-7 Member of Triassic Yanchang Formation) of the YC23 Well in the Ordos Basin as the research object, this study attempts to obtain a full understanding of the distribution characteristics of different gas components, to explore the migration ability of different gas components, and to explain the accumulation characteristics of shale gas.

In 2011, the first vertical shale gas well in the Ordos Basin, the Liuping 177 well, penetrated Chang-7 shale and produced shale gas with a daily production rate of 700–1500 m³/day. Since then, dozens of horizontal wells have been drilled and evaluated. However, the shale gas production was far less than expected and new drilling has essentially stopped. Most of the geologists believe that the low thermal maturity of Chang-7 shale, which is only in the oil generation window, is the primary reason for the poor shale gas resources. However, the high organic abundance of Chang-7 shale is suitable for carrying out the gas desorption and related experiments. Thus, the exploration and development of shale gas in the Ordos Basin has promoted the scientific research on shale gas.

2. Geological Background

The Ordos Basin is the second largest basin in China and covers an area of 37×10^4 km² [11]. The basin is located west of the North China Platform and is bounded by the Qilian–Qinling collision zone in the southwest, the Liupanshan Basin in the west, the Alashan Platform in the northwest, the Hetao Graben in the north, the Luliang Uplift in the east, and the Fenwei Graben in the south (Figure 1) [20,21]. In the central-southern part of the Ordos Basin, the Triassic Yanchang Formation, which contains 10 members (i.e., Chang-1, Chang-2, ..., Chang-9, Chang-10), was deposited in a lacustrine environment. The organic-rich shale is developed within the Chang-7 and Chang-9 members. The Chang-7 Member, with the Chang-7₁, Chang-7₂, and Chang-7₃ sub-layers, contains 20–200 m (65–650 ft) thick shale. As most of the shale deposits are within Chang-7₂ and Chang-7₃ sub-layers, the commonly named Chang-7 shale represents Chang-7₂ shale and Chang-7₃ shale. The Chang-7 shale has a shallow burial depth of 700–2400 m (2300–7800 ft), and high organic abundance, with an average TOC of more than 3.8% [22,23].

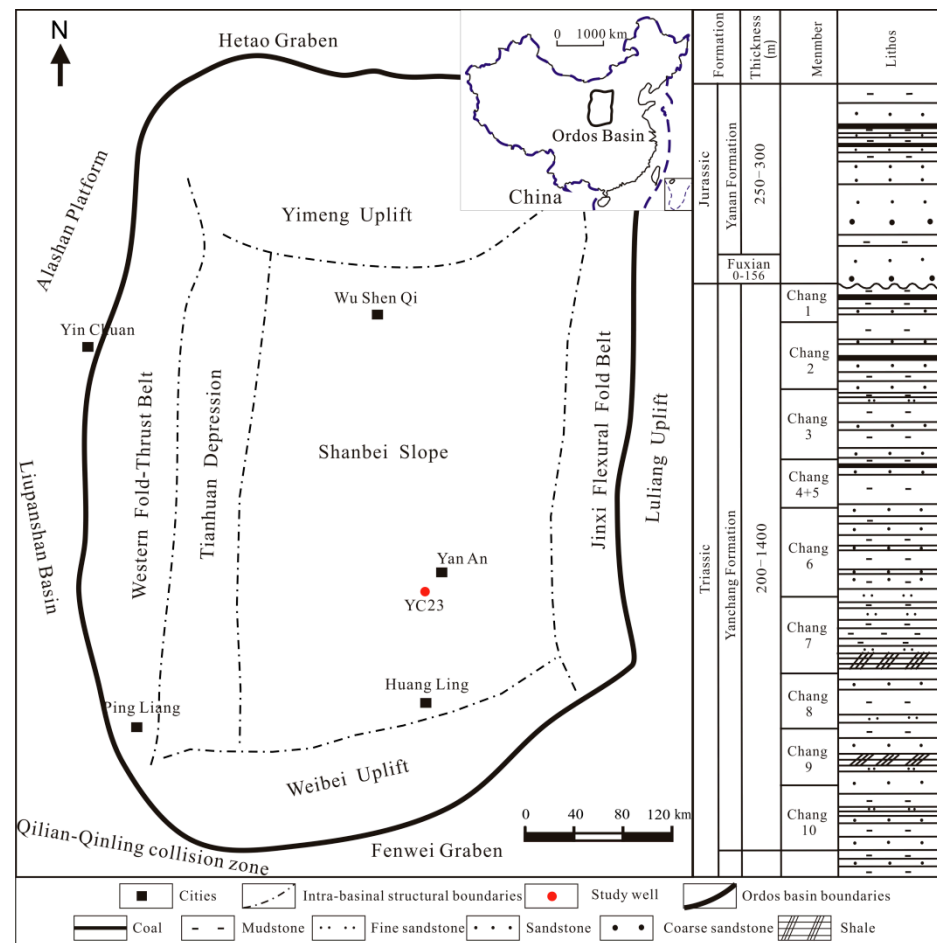


Figure 1. Map showing the stratigraphic succession of Ordos Basin and the location of the study well.

3. Sampling and Experiments

Nineteen Chang-7 shale (Chang-7₃) samples were collected from the YC23 Well (Figure 2). Total organic carbon content and gas desorption experiments were carried out for 19 samples, and rock pyrolysis were carried out for 13 samples. For the desorbed gas, gas chromatography was conducted to obtain the contents of different gas components. In addition, carbon isotope testing was carried out for the desorbed gas collected from 14 samples. The workflow and purpose of the experiments are shown in Figure 2.

Conventional coring was used in the YC23 Well. It took 30–45 min for the cores to be pulled to the surface. It should be noted that a certain amount of gas was lost during the drilling and sampling processes. Firstly, the temperature–pressure balance of the oil–gas–water system is damaged when the drilling bit penetrates the shale, leading to loss of gas even though the borehole is filled with drilling fluid. Secondly, a decrease in temperature and pressure when the core is pulled up to the surface could also result in gas loss. Several methods for calculating lost gas have been proposed as discussed in the introduction. However, it is very difficult to obtain the accurate quantity of lost gas. Moreover, the lost volumes of different gas components’ carbon isotopes are still not fully understood. In order to avoid gas losses, all the desorption experiments in this study were carried out in the Coring well site. The sample must be cleaned and broken before the desorption experiments; thus, it took 5–10 min for the cores to be placed in the desorption canisters at the site. In addition, the main focus of this study is the differences in the content of the gas components, thus the lost gas has not been considered.

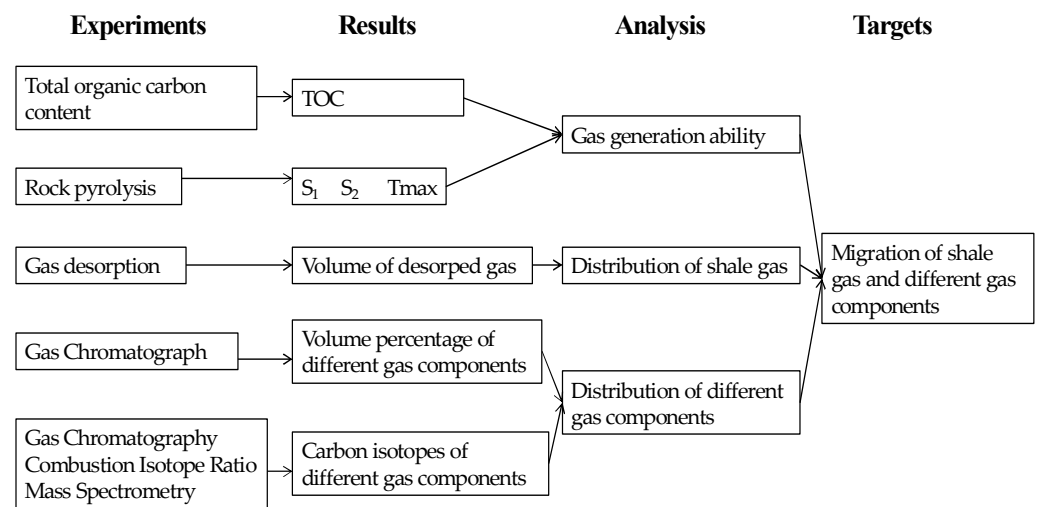


Figure 2. Chart showing the workflow and purpose of experiments.

The total organic carbon content was measured using Vario TOC. The experimental procedures were as follows: (1) the solid rock was milled into powder of less than 100 mesh; (2) hydrochloric acid solution (5% dilute) and powder samples were placed in the fume hood for ventilation (three days) to remove carbonate; (3) the samples were placed in the incubator (50 °C) to dry (three days); (4) the samples were packed in tin foil after being weighed; and (5) the samples were placed and the instrument was started. The Vario TOC automatically compares the sample with a standard sample based on the detected peak area and determines the organic carbon content.

Rock-eval was used for rock pyrolysis. The experimental procedures were as follows: (1) the rock samples were broken and each weighed about 100 mg for the experiment; (2) the sample was heated at a temperature of 300 °C for 3 min, and then heated to 650 °C at a heating rate of 25 °C/min. The measured parameters included free hydrocarbon (S_1), pyrolysis hydrocarbon (S_2) and maximum pyrolysis temperature (Tmax).

The SH-C01 desorption system was used for the shale gas desorption experiment. The experimental procedures were as follows: (1) the fresh shale samples were placed in the sealed tank and fill it with helium; (2) the sealed tank was placed on the centrifugal table to centrifuge the shale into powder; (3) the sealed tank was placed into the desorption system and heated for 3 h (120 °C, as nearly all the adsorbed gases can be desorbed near 120 °C) [4]. The procedure for gas collection was as follows: (1) the measuring cylinder (with a semi-closed end controlled by a valve and an open end) was put in a water pot and filled with water; (2) the measuring cylinder was kept below the water surface; (3) the valve of the upper end was closed; (4) the hose (which connects the SH-C01 desorption system) was put near the lower open end of the measuring cylinder; (5) this made the desorbed gas flowing into the measuring cylinder; and (6) the desorbed gas was collected from the upper end through the valve.

The gas components were measured using a gas chromatograph (Agilent 6890N). The experimental conditions were as follows: GDX-502 chromatographic column (3 mm × 4 m), mesoporous molecular sieve (3 mm × 2.4 m), and capillary chromatogram column (50 m × 0.53 mm). The temperature of the chromatographic column ranged from 30 °C to 160 °C (with a heating rate of 70 °C/min). The pressure of the chromatographic column was 200 KP. The carrier gas was helium. The injection temperature of the chromatographic column was 120 °C. The quantity of injected sample gas was 1 mL. The detection limit ranged from 0.1 ppm to 10 ppm. The measuring accuracy was about ±5%.

The carbon isotopic composition was measured using gas chromatography combustion isotope ratio mass spectrometry (GC-C-IRMS). In the GC-C-IRMS system, the gas chromatography instrument is HP6890I (Agilent Technologie, Santa Clara, CA, USA), and isotopic mass spectrometer instrument is Finigan Delta plus XP (Thermo Finigan, San Jose,

CA, USA). During the testing, the separated compound was burned and converted into carbon dioxide in a combustion furnace for carbon isotopic composition analysis. The chromatographic column used was CP-CarboBOND (25 m × 0.53 mm × 10 μm). Chromatography heating was performed by keeping the initial temperature at 30 °C for 5 min, increasing the temperature to 240 °C with a heating rate of 15 °C/min, and keeping the temperature at 240 °C for 10 min. The flow rate of the carrier gas (helium gas) was kept at 6.2 mL/min. The accuracy of the measured carbon isotopes was about ±0.3‰.

4. Experimental Results

The desorption tests and TOC tests were conducted for 19 shale samples from the study area. The TOC in the Chang-7 shale ranges from 0.68% to 8.52%, with an average value of 4.06%, indicating that the organic matter abundance in Chang-7 shale is high. Among the measured shale samples, 31.5% of the samples (6 samples) have TOC < 2%; 42.1% of the samples (8 samples) have 2% < TOC < 6% and 26.4% (5 samples) of the samples have TOC > 6%. The S₁ ranges from 0.88 to 8.72 mg/g, with an average value of 3.66 mg/g; the S₂ ranges from 0.66 to 24.48 mg/g, with an average value of 8.05 mg/g; the Tmax ranges from 446 to 459 mg/g, with an average value of 454 mg/g. The volume of desorbed gas ranges from 0.6 to 2.32 m³/t, with an average value of 1.26% (Table 1). Compared with most marine shale systems, the shale gas content of Chang-7 shale is generally at a medium or low level [3].

Table 1. Basic parameters of shale samples.

Samples	Burial Depth (m)	S ₁	S ₂	TOC (%)	Tmax (°C)	HI	Desorbed Gas m ³ /t
S1	1405.13	-	-	5.37	-	198.51	1.41
S2	1405.64	5.14	10.3	5.48	446	187.96	1.78
S3	1406.97	2.64	11.56	6.83	455	169.25	1.84
S4	1407.75	5.67	15.83	6.37	448	248.51	1.29
S5	1408.44	-	-	8.15	-	219.02	2.32
S6	1410.56	8.72	24.48	8.01	454	305.62	2.09
S7	1411.27	6.78	10.23	8.52	455	202.23	1.98
S8	1415.22	-	-	2.69	-	105.95	1.48
S9	1417.16	2.85	6.04	2.35	452	257.02	1.36
S10	1424.27	3.14	4.49	3.66	456	122.68	0.94
S11	1424.78	-	-	3.48	-	180.17	0.71
S12	1425.13	1.13	8.06	4.03	458	200.00	1.05
S13	1429.46	2.48	1.8	1.89	447	95.24	0.66
S14	1432.34	-	-	1.84	-	96.20	1.04
S15	1432.54	2.4	5.17	4.88	455	105.94	1.12
S16	1434.73	-	-	1.32	-	13.64	0.85
S17	1436.85	3.36	4.79	0.68	459	704.41	0.71
S18	1437.56	2.33	1.84	0.72	457	255.56	0.60
S19	1440.23	0.88	0.06	0.96	455	6.25	0.78

S₁: free hydrocarbons; S₂: pyrolysis hydrocarbons; Tmax: maximum pyrolysis temperature; HI: hydrogen index.

The desorbed gas from the Chang-7 shale samples mainly contains four types of gas components, including methane (C₁), heavy gases (C₂—ethane; C₃—propane; iC₄—iso-butane; nC₄—n-butane; iC₅—iso-pentane; nC₅—n-pentane), carbon dioxide (CO₂) and nitrogen (N₂) (Figure 3). Among the measured shale samples, the volume percentage of CH₄ ranges from 22.89% to 85.95%, with an average value of 52.16%; the volume percentage of C₂H₆ ranges from 1.95% to 34.37%, with an average value of 20.45%; the volume percentage of propane ranges from 0.7% to 17.47%, with an average value of 8.71%; the volume percentage of C₃H₈ (n-butane and iso-butane) ranges from 0.6% to 7.58%, with an average value of 4.01%; the volume percentage of pentane (n-pentane and iso-pentane) ranges from 0.0% to 2.53%, with an average value of 1.13%; the volume percentage of carbon dioxide ranges from 0.0% to 16.66%, with an average value of 5.69%; and the volume percentage of nitrogen ranges from 0.0% to 28.8%, with an average value of 7.85%.

Among the four types of gas components, the CH₄ content is relatively high, followed by heavy gases, while the content of carbon dioxide and nitrogen are relatively low.

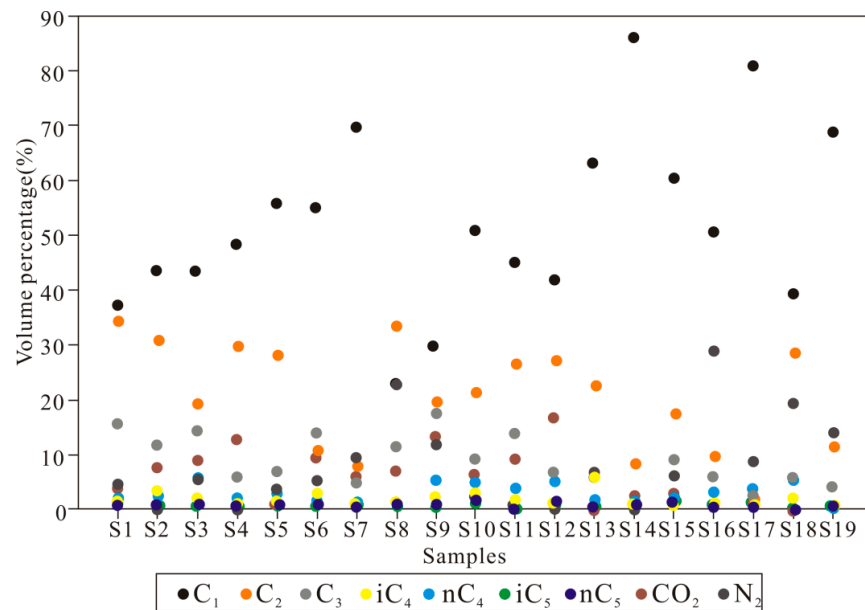


Figure 3. The volume percentage of different gas components. C₁: methane; C₂: ethane; C₃: propane; iC₄: iso-butane; nC₄: n-butane; iC₅: iso-pentane; nC₅: n-pentane; CO₂: carbon dioxide; N₂: nitrogen.

Carbon isotopes tests were conducted for 14 shale samples in the study area (Figure 4). The test results showed that the methane carbon isotopes ($\delta^{13}C_1$) range from -52.8‰ to -44.1‰ , with an average value of -48.97‰ ; the ethane carbon isotopes ($\delta^{13}C_2$) range from 41.3‰ to -35.6‰ , with an average value of -38.37‰ ; the propane carbon isotopes ($\delta^{13}C_3$) range from -38.6‰ to -31.8‰ , with an average value of -33.32‰ ; the butane carbon isotopes range from -34.8‰ to -24.8‰ , with an average value of -29.56‰ ; the dioxide carbon isotopes range from -20.1‰ to -16.2‰ , with an average value of -17.94‰ . However, it should be noted that some samples do not contain carbon isotopes for C₃H₈, iC₄ and CO₂.

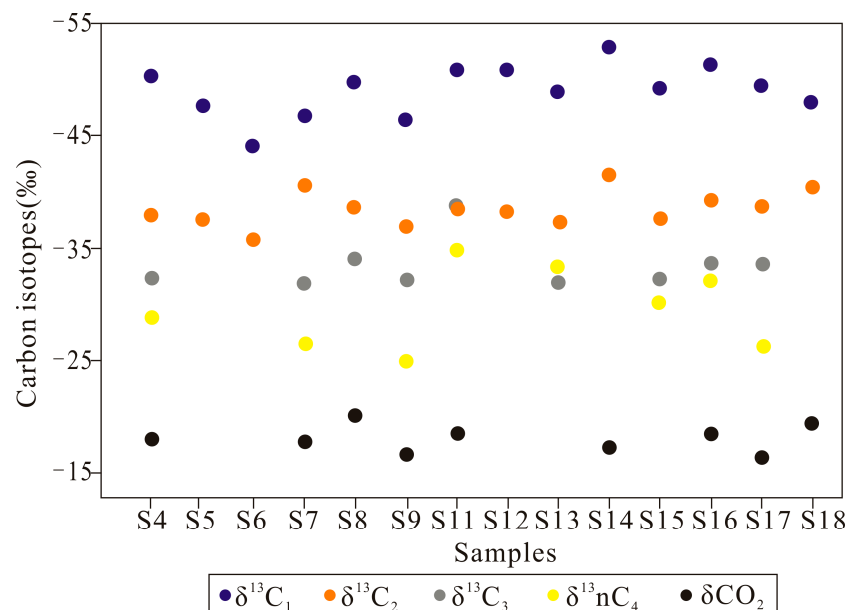


Figure 4. The carbon isotopes of different gas components. $\delta^{13}C_1$: methane carbon isotopes; $\delta^{13}C_2$: ethane carbon isotopes; $\delta^{13}C_3$: propane carbon isotopes; $\delta^{13}nC_4$: n-butane carbon isotopes; δCO_2 : carbon dioxide carbon isotopes.

5. Origins of Shale Gas Sampling

Gaseous hydrocarbon components such as R , $R = C_1/(C_2 + C_3)$, and $\delta^{13}C_1$ are important parameters for assessing the gas origins. The R value for gas of thermal origin is normally less than 100, and the $\delta^{13}C_1$ is normally larger than -55‰ [24]. In this study, the R values range from 0.51 to 17.69, with an average value of 3.14; the $\delta^{13}C_1$ are larger than -55‰ (Figure 5). Thus, it can be inferred that the Chang-7 shale gas is of thermal origin. The above viewpoint is also proved by the thermal maturity of the study area. The thermal maturity of Chang-7 shale in the study area is generally in the oil generation window (vitrinite reflectance ranges from 0.8% to 1.1%) [25,26]. Thus, the Chang-7 shale gas collected from the YC23 Well is of thermal origin, though some Chang-7 shale gas in the Ordos Basin is biogas [4,5].

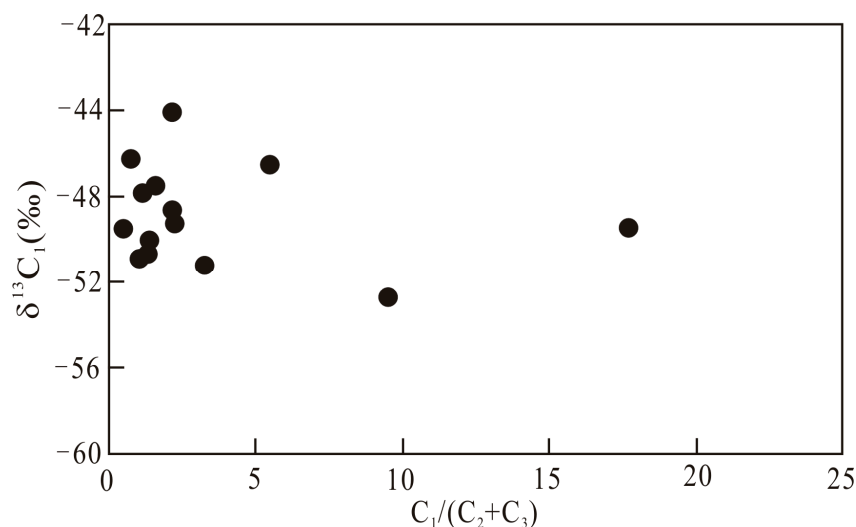


Figure 5. Cross plots of $C_1/(C_2 + C_3)$ vs $\delta^{13}C_1$.

Normally, $\delta^{13}C_1$ becomes heavier with increasing thermal maturity, and it is always characterized by the distinctive fractionation phenomenon. Thus, $\delta^{13}C_1$ is a reliable index for judging the maturity of natural gas [13,27,28]. The heavy gases usually evolved from kerogen or crude oil during thermal evolution, and it is always characterized by the minor fractionation phenomenon. For example, the carbon isotopes of some heavy gases, including $\delta^{13}C_2$ and $\delta^{13}C_3$ have a narrow fractionation range, and their values are close to the carbon isotopes of the parent material. Thus, the carbon isotopes of heavy gases are an effective index for inferring the genesis of the shale gas. The typical oil-type gas that is distributed across the world has the following characteristics: $-55\text{‰} < \delta^{13}C_1 < -30\text{‰}$; $\delta^{13}C_2 < -28.8\text{‰}$; $\delta^{13}C_3 < -25.5\text{‰}$; and $\delta^{13}C_{CO_2} < -10\text{‰}$ [29,30]. The desorbed gas from Chang-7 shale has the following characteristics: $-52.8\text{‰} < \delta^{13}C_1 < -44.1\text{‰}$; $\delta^{13}C_2 < -33.6\text{‰}$; $\delta^{13}C_3 < -31.8\text{‰}$; and $\delta^{13}C_{CO_2} < -16.2\text{‰}$. The features mentioned above proved that the Chang-7 shale gas in this area is an oil-type gas (Figure 6).

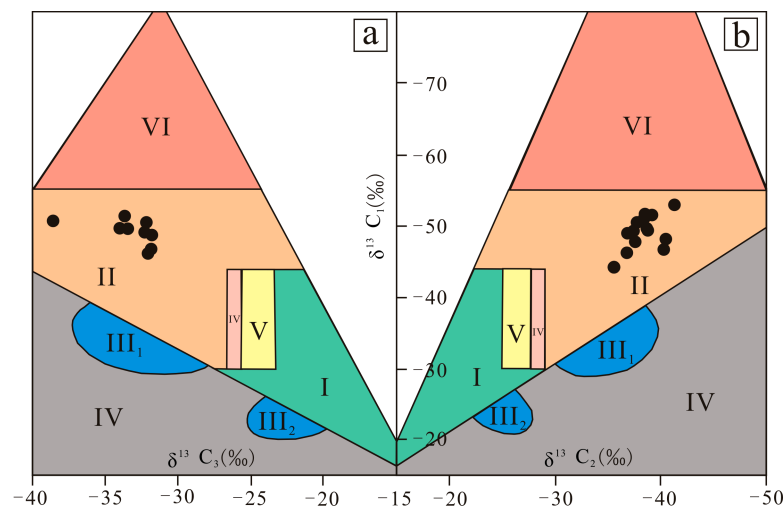


Figure 6. Cross plots of carbon isotope (a) CH_4 versus C_2H_6 ; (b) CH_4 versus C_3H_8 . I—coal-type gas; II—oil-type gas; III—carbon isotope inversion gas; IV—humic and sapropelic gas; V—mixture of coal-type and oil-type gas; VI—biogas and sub biogas.

6. Discussion

The Chang-7 shale system has very strong lithologic heterogeneity, and it contains a large number of sandy laminae and thin sandstone layers. The YC23 Well is a representative well that reflects lithologic heterogeneity (Figure 7). In the depth range of 1400–1418 m (4592–4651 ft), the lithology is dark shale with limited sandy laminae. In the depth range of 1418–1445 m (4651–4739 ft), the lithology is a good combination of dark shale, sandy laminae, and thin sandstone layers. Some former studies have proved that the existence of lithologic heterogeneity could cause serious heterogeneity in both the organic geochemistry and the reservoir characteristics, which could affect the generation, migration and distribution of shale gas [21]. The YC23 Well completely substantiates the above viewpoint. In regard to the YC23 Well, the volumes of desorbed shale gas, S_2 , and TOC are extremely high in the depth range of 1400–1418 m (4592–4651 ft) (the section of thick, dark shale), and the volumes of desorbed shale gas, S_2 , and TOC are low in the depth range of 1418–1445 m (4651–4739 ft) (the combined shale, sandy laminae, and thin sandstone layers) (Figure 7).

6.1. Classification of Generated Gas, Retained Gas and Migrated Gas

As shale with the ability to generate large amounts of gas usually has a larger TOC, S_1 and S_2 , this study used TOC, S_1 and S_2 to assess the generated gas. As shale gas can migrate, this may cause component fractionation; thus, this study used component fractionation to distinguish the retained gas and migrated gas (Figure 8).

The test results from 19 shale samples from the YC23 Well show that the TOC is closely related to the generation, migration and occurrence of shale hydrocarbon. S_1 is the liquid-free hydrocarbon in shale, which roughly represents the shale oil generated and stored in the shale system. However, hydrocarbons can easily migrate along pores and micro-fractures; thus, S_1 often does not represent in situ-generated shale oil, but retained or stored oil after migration. For shale samples with a TOC less than 6% in the YC23 Well, there is no positive correlation between TOC and S_1 , indicating that shale oil in such samples has undergone large-scale migration (Figure 9a). S_2 roughly represents the hydrocarbon generation ability of the low–medium maturity source rock, and the volume of desorbed gas roughly represents the ability to generate shale gas. In the YC23 Well, the TOC shows a good positive correlation with S_2 and the volume of desorbed gas (Figure 9b,d). Thus, it can be inferred that shale with higher TOC in the YC23 Well has a stronger gas generation ability. For shale samples with TOC less than 6% in the YC23 Well, there is a weak positive correlation between desorbed gas and TOC, and there is no correlation between desorbed

gas and S_1 . The abovementioned phenomena indicate that shale gas in the shale samples with TOC less than 6% has also experienced gas migration (Figure 9c,e).

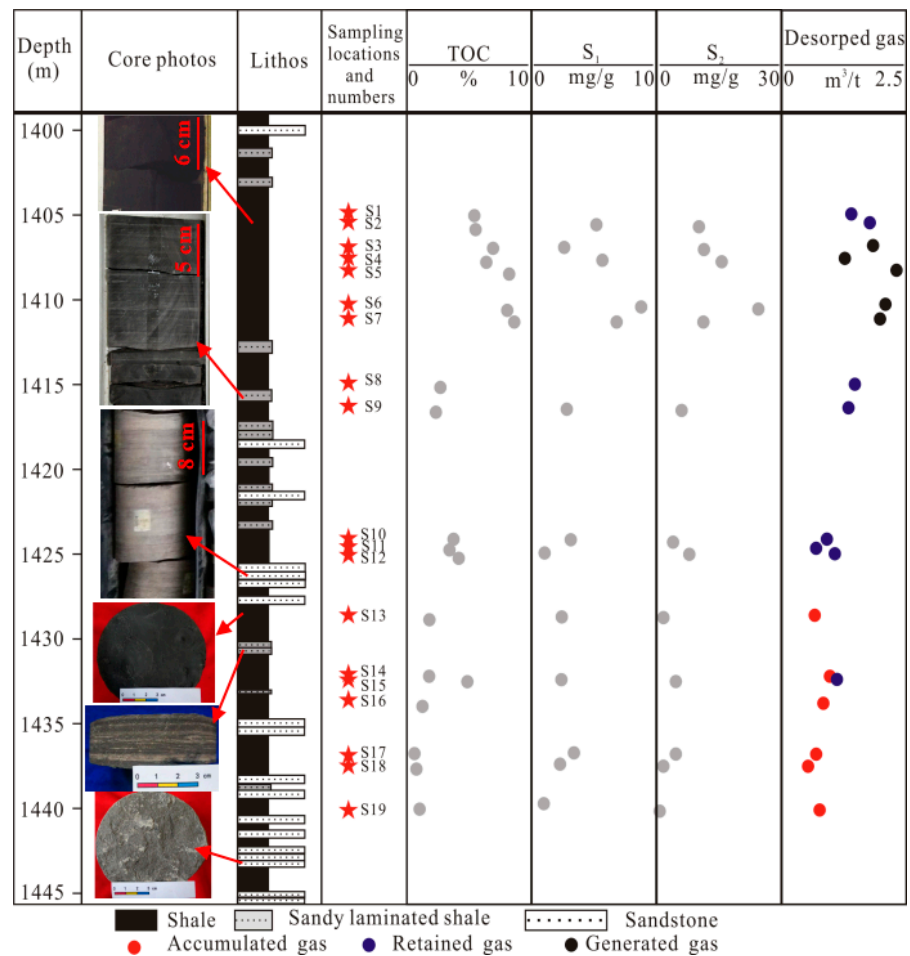


Figure 7. Histogram showing the cores, geological parameters and gas-type classifications.

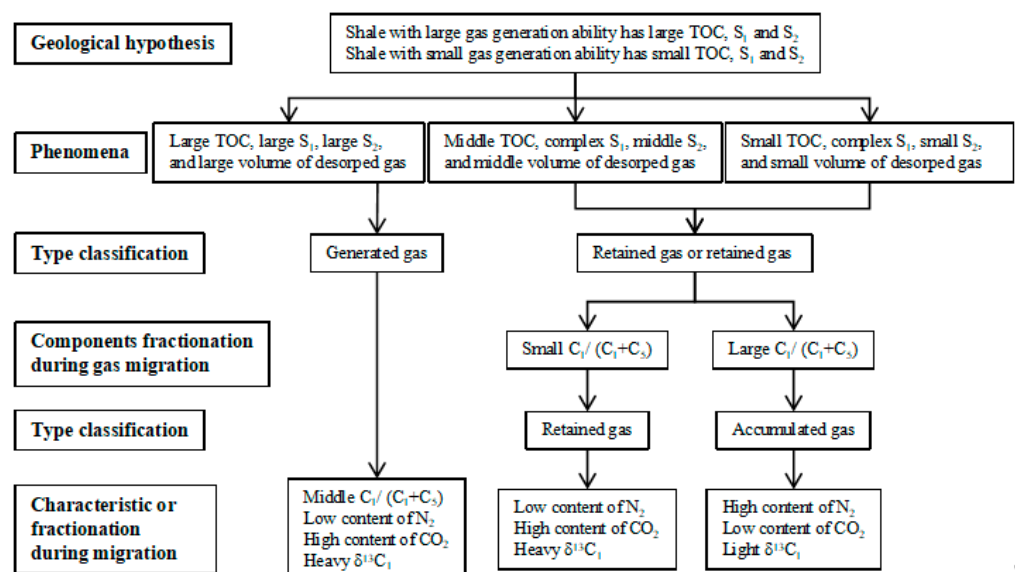


Figure 8. Chart showing classification of gas types.

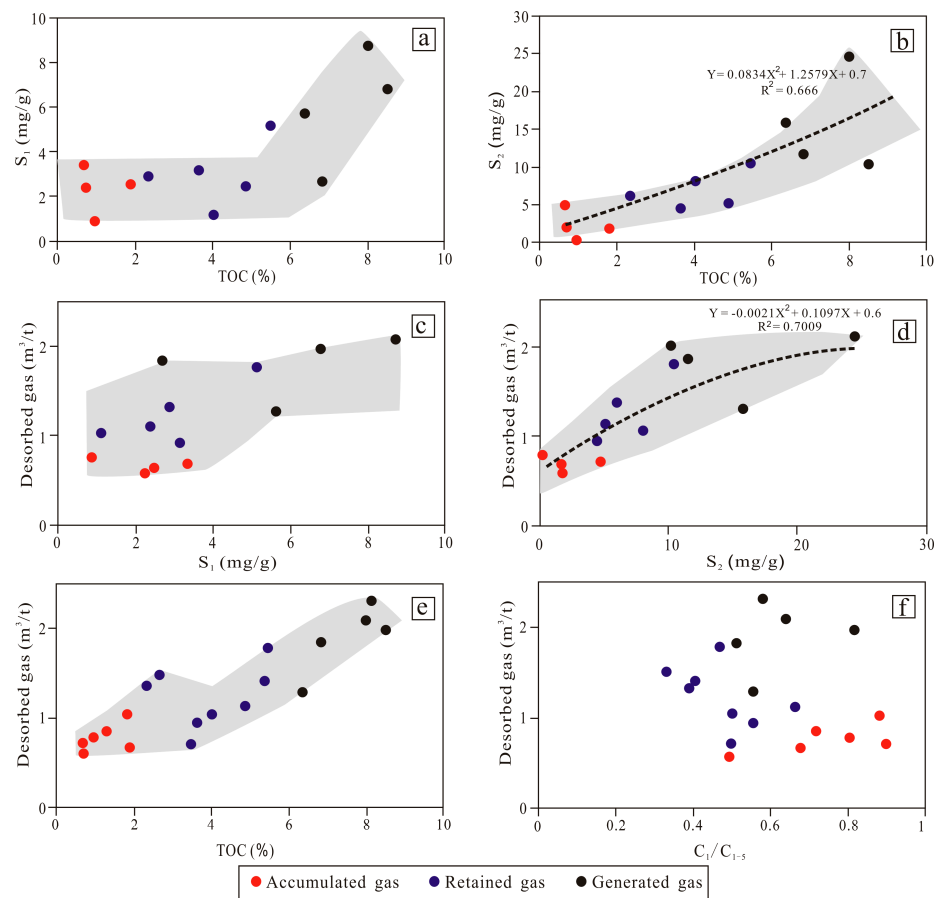


Figure 9. Parameter characteristics for classifying shale gas. (a) Relationship between TOC and S_1 ; (b) Relationship between TOC and S_2 ; (c) Relationship between desorbed gas and S_1 ; (d) Relationship between desorbed gas and S_2 ; (e) Relationship between desorbed gas and TOC; (f) Relationship between desorbed gas and C_1/C_{1-5} .

For shale samples with TOC less than 2%, however, the volume of desorbed gas is low (between 0.6 and 1.03 m³/t, the average content is 0.77 m³/t), and the gas dryness is high (between 0.49 and 0.89, the average value is 0.74); For shale samples with TOC between 2% and 6%, the volume of desorbed gas is medium (between 0.71 and 1.78 m³/t, the average content is 1.23 m³/t), and the gas dryness is low (between 0.33 and 0.66, the average value is 0.48); For shale samples with TOC larger than 6%, the volume of desorbed gas is high (between 1.28 and 2.31 m³/t, the average content is 1.90 m³/t), and the gas dryness is high (between 0.50 and 0.82, the average value is 0.62) (Figure 9e,f). As shale with low TOC usually has low hydrocarbon generation ability, the shale samples with TOC less than 2% may generate a small amount of shale gas, resulting in the low volume of desorbed gas. However, the low volume of desorbed gas does not indicate that the shale gas is in situ-generated gas, because a part of the gas generated by shale with higher TOC may migrate and be store within the samples with TOC less than 2%. In order to assess the in situ-generated gas or migrated gas, the gas dryness can be used as a reference. Generally, there is no correlation between the gas volume and the gas dryness, or there is no significant difference in the gas dryness. However, samples with different TOC ranges in the study area have significant differences in gas dryness. Shale samples with TOC between 2% and 6% have the minimum value of gas dryness; shale samples with TOC less than 2% have the maximum value of gas dryness; shale samples with TOC larger than 6% have a medium value of gas dryness. Since the migration ability of CH₄ is stronger than that of heavy hydrocarbon gases, the fractionation is likely caused by gas migration.

Based on the geological characteristics of shale and shale gas, the shale gas desorbed from different shale samples in the YC23 Well can be defined as three types, namely,

generated gas, retained gas and accumulated gas (Figures 7 and 9) (Table 2). By comparing the difference in the components of the generated gas, retained gas and accumulated gas, the shale gas migration and occurrence characteristics can be fully analyzed.

Table 2. Shale gas classification based on gas generation, migration and distribution.

Types	Shale and Shale Gas Characteristics						
	Shale Thickness	Locations	TOC	Desorbed Gas (Average Value)	Volume of Generated Gas	Volume of Migrated Gas	Generated Gas or Migrated Gas
Generated gas	18 m	Middle part of thick shale	>6%	Large (3.80 m ³ /t)	Large	No or small	In situ-generated gas
Retained gas	-	Margin parts of thick shale or thin shale	2%~6%	Middle (2.45 m ³ /t)	Large	Large	Part of in situ generated gas
Accumulated gas	<5 m	Thin shale	<2%	Small (1.54 m ³ /t)	Small	No or small	In situ-generated gas and migrated gas

The generated gas has the following characteristics: (1) shale gas is located in the middle part of thick high-quality shale (about 18 m or 59 ft thick, TOC larger than 6%); (2) shale samples that host generated gas are able to generate large amounts of gas and the volume of desorbed gas is large; (3) the generated gas has no migration or weak migration; and (4) the shale gas is mainly in situ-generated gas.

The retained gas has the following characteristics: (1) shale gas is located in the thin shale and marginal parts of thick shale (TOC is between 2% and 6%); (2) shale samples that host retained gas have medium gas generation ability and the volume of desorbed gas is medium; (3) part of the generated gas migrates out of shale; and (4) the shale gas is only partly in situ generated gas.

The accumulated gas has the following characteristics: (1) shale gas is located in thin shale (TOC less than 2%); (2) shale samples that host accumulated gas have a small gas generation ability and the volume of desorbed gas is small; (3) the generated gas has no migration or weak migration; and (4) the shale gas is a mixture of in situ-generated gas and migrated gas.

6.2. Migration of Different Gas Components

In the burial depth range of 1400–1418 m (4592–4651 ft) of the YC23 Well, the heterogeneity of the shale system is very weak (only a small amount of sandy lamina is contained therein), and the TOC values are extremely high. In the shale section of 1400–1418 m (4592–4651 ft), the volume of desorbed gas is relatively high compared with other sections with highly developed sandy lamina or sandstone (Figure 5). Thus, it can be inferred that the volume of desorbed gas in thick shale is large and that in thin shale is small. The abovementioned characteristics are likely to indicate that the shale gas in the thick shale has difficulty migrating, while the shale gas in the thin shale migrates easily. In fact, whether it is a marine sedimentary system or lacustrine sedimentary system, oil and gas migrate easily due to the improved seepage conditions (the effective contact between thin shale and sandstone can improve the seepage conditions); however, oil and gas have difficulty migrating within thick shale due to poor seepage conditions [10,31,32].

The CH₄ content of the accumulated gas in the YC23 Well ranges from 39.31% to 85.95% (average content of 64.73%). The CH₄ content of the retained gas ranges from 22.89% to 60.36% (average content is 41.35%). The CH₄ content of the generated gas ranges from 43.30% to 69.59% (average content of 54.39%). The content of heavy gases in the accumulated gas of the YC23 Well ranges from 9.28% to 41.29% (an average content of 21.58%). The content of heavy gases in the retained gas ranges from 30.66% to 54.67% (average content is 44.38%). The content of heavy gases in the generated gas ranges from 15.07% to 42.45% (average content is 33.41%) (Figure 10a,b). It can be inferred that the accumulated gas has the highest content of CH₄ and the lowest content of heavy gases; the

generated gas has the medium content of CH_4 and the medium content of heavy gases; the retained gas has the lowest content of CH_4 and the highest content of heavy gases.

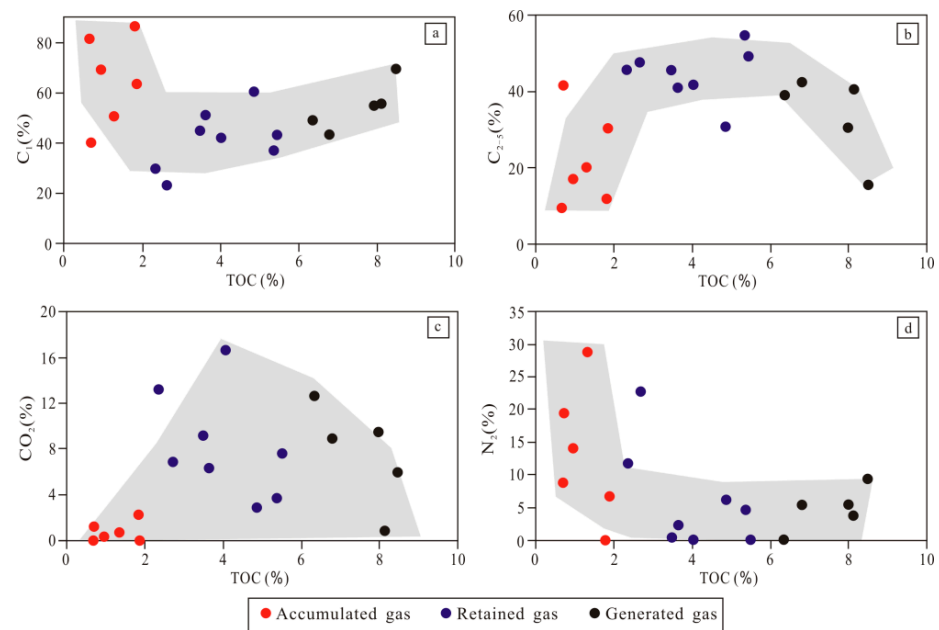


Figure 10. Relationship between TOC and different gases. (a) Relationship between CH_4 and TOC; (b) Relationship between heavy gases and TOC; (c) Relationship between CO_2 and TOC; (d) Relationship between N_2 and TOC.

Since the migration ability of CH_4 is stronger than that of heavy hydrocarbon gases under the same geological conditions, the difference in the content of CH_4 and heavy gases can be used to confirm the migration status [33,34]. For accumulated gas, the shale gas desorbed from low organic shale ($\text{TOC} < 2\%$). The most likely reason for the high content of CH_4 and low content of heavy gases is that some CH_4 underwent gas migration and was then stored with the in situ-generated gas. For the retained gas, the shale gas desorbed from medium organic shale ($2\% < \text{TOC} < 6\%$). The most likely reason for the low content of CH_4 and high content of heavy gases is that some CH_4 underwent gas migration and then parts of the in situ-generated gas were stored. For the generated gas, the shale gas desorbed from high organic shale ($\text{TOC} > 6\%$). The content of CH_4 and heavy gases are at a medium level due to minor gas migration or no migration.

The CO_2 content of the accumulated gas in the YC23 Well ranges from 0.00% to 2.30% (average content of 0.75%). The CO_2 content of the retained gas ranges from 2.82% to 16.66% (average content of 8.30%); and the CO_2 content of the generated gas ranges from 0.62% to 12.53% (average content of 7.46%). The N_2 content of the accumulated gas ranges from 0.00% to 28.80% (average content of 12.95%); the N_2 content of retained gas ranges from 0.00% to 22.71% (average content of 5.97%); and the N_2 content of the generated gas ranges from 0.00% to 9.43% (average content of 4.75%) (Figure 10c,d). It can be inferred that the CO_2 content of accumulated gas is very low, and the CO_2 content of generated gas and retained gas is very high; the N_2 content of accumulated gas is very high; and the N_2 content of generated gas and retained gas is very low.

Both the mineral particles and the kerogen have stronger adsorption ability for CO_2 compared with N_2 ; therefore, N_2 migrates easily and the migration of CO_2 is very difficult in the shale system [6,7,9,35,36]. Thus, the difference in the content of CO_2 and N_2 can be used to confirm the shale gas migration. For the accumulated gas, the high content of N_2 is probably caused by gas migration as the N_2 has a strong migration ability whereas CO_2 has a weak migration ability. Similarly, a large amount of N_2 underwent migration; thus, the retained gas has a lower content of N_2 and a higher content of CO_2 .

For the accumulated gas in the YC23 Well, the content of N_2 and CH_4 ranges from 58.71% to 89.51% (average content of 77.67%); the content of heavy gases ranges from 9.28% to 41.29% (average content of 21.58%); and the content of CO_2 ranges from 0.00% to 2.30% (average content of 0.75%). For the retained gas in the YC23 Well, the content of N_2 and CH_4 ranges from 41.23% to 66.51% (average content of 47.32%); the content of heavy gases ranges from 30.66% to 54.67% (average content of 44.38%); and the content of CO_2 ranges from 2.82% to 16.66% (an average content of 8.30%). For the generated gas in the YC23 Well, the content of N_2 and CH_4 ranges from 48.58% to 79.02% (average content of 59.13%); the content of heavy gases ranges from 15.07% to 42.45% (average content of 33.41%); and the content of CO_2 ranges from 0.62% to 12.53% (average content of 7.46%). On the ternary plots of the gas components, the accumulated gas samples are mainly distributed in the upper left corner of the chart, the retained gas samples are mainly distributed in the lower left corner of the chart, and the generated gas samples are mainly distributed in the middle of the chart (Figure 11). Thus, it can be inferred that each different gas component has a unique migration ability, and as a result, the accumulated gas, retained gas and generated gas have different component contents.

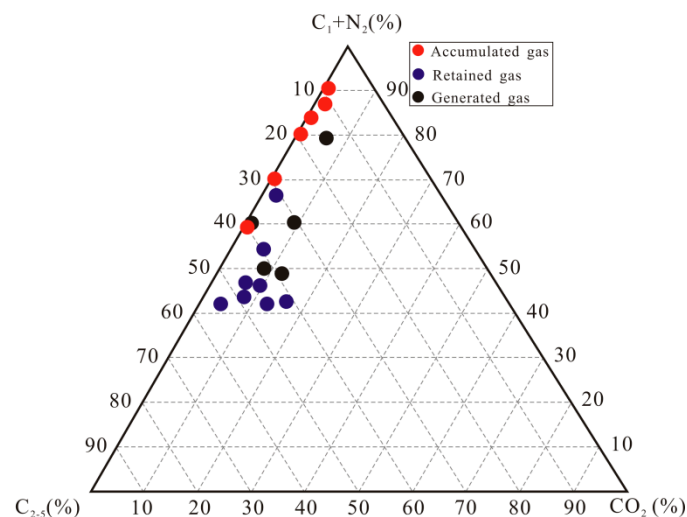


Figure 11. Ternary plots of $N_2 + CH_4$, CO_2 and heavy gases.

For the accumulated gas in the YC23 Well, the value of $\delta^{13}C_1$ ranges from -50.06‰ to -47.9‰ (average value of -52.8‰), and the value of $\delta^{13}C_2$ ranges from -39.3‰ to -37.1‰ (average value of -41.3‰). For the retained gas in the YC23 Well, the value of $\delta^{13}C_1$ ranges from -49.36‰ to -46.3‰ (average value of -50.9‰), and the value of $\delta^{13}C_2$ ranges from -37.88‰ to -36.7‰ (average value of -38.6‰). For the generated gas in the YC23 Well, the value of $\delta^{13}C_1$ ranges from -47.13‰ to -44.1‰ (average value of -50.2‰), and the value of $\delta^{13}C_2$ ranges from -37.83‰ to -35.6‰ (average value of -40.3‰) (Figure 12a,b). It can be inferred that the accumulated gas has relatively light $\delta^{13}C_1$ values and $\delta^{13}C_2$ values, and the retained gas and the generated gas have relatively heavy $\delta^{13}C_1$ values and $\delta^{13}C_2$ values. During the gas migration process, $\delta^{13}C_1$ is one of the easiest components to migrate compared with other carbon isotopes including $\delta^{13}C_2$, $\delta^{13}C_3$, δCO_2 . Thus, it is easy to show a migration fractionation for $\delta^{13}C_1$ during gas migration [37–39]. Therefore, the $\delta^{13}C_1$ values can be used as indicators to assess gas migration. For the accumulated gas, there must be more gas with relatively light $\delta^{13}C_1$, as $\delta^{13}C_1$ migrates more easily compared with other carbon isotopes. In addition, there is little difference in $\delta^{13}C_2$ in the retained gas and the generated gas, although the accumulated gas has a relatively light weight $\delta^{13}C_2$ value (Figure 12b). Thus, it can be inferred that the difference in the $\delta^{13}C_2$ value is probably not caused by gas migration, but by the gas generation, because different shale samples have difference gas generation abilities.

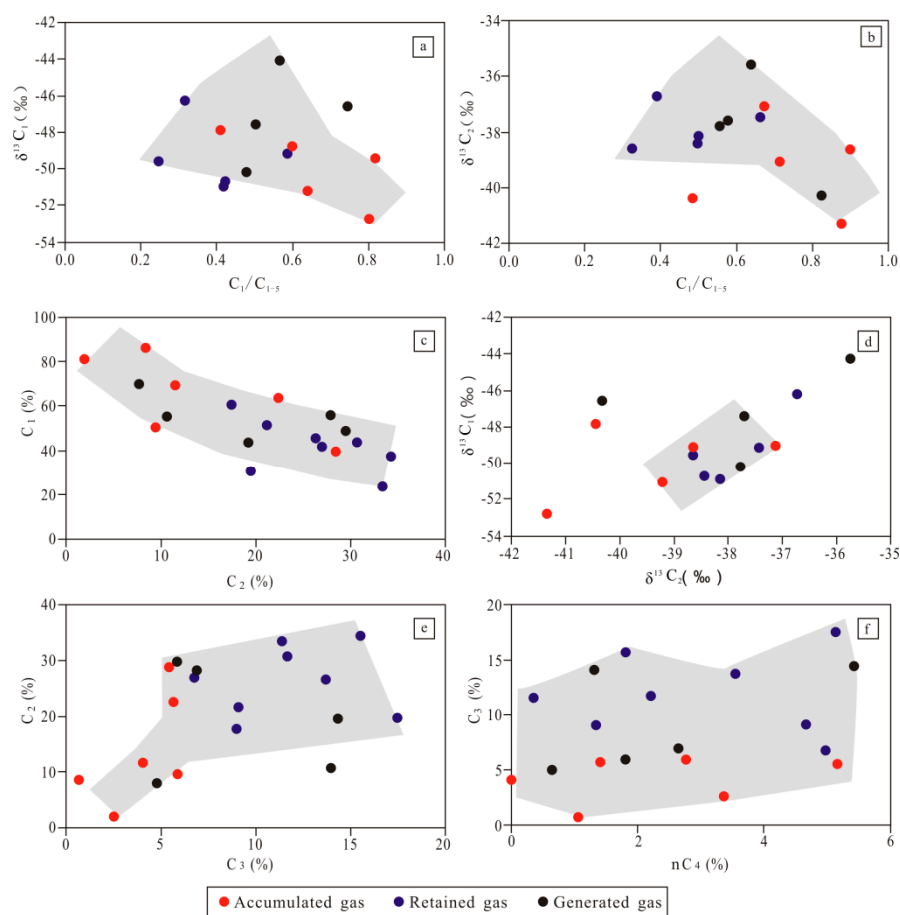


Figure 12. The fractionation of different gas components. (a) Relationship between $\delta^{13}\text{C}_1$ and C_1/C_{1-5} ; (b) Relationship between $\delta^{13}\text{C}_2$ and C_1/C_{1-5} ; (c) Relationship between C_1 and C_2 ; (d) Relationship between $\delta^{13}\text{C}_1$ and $\delta^{13}\text{C}_2$; (e) Relationship between C_2 and C_3 ; (f) Relationship between C_3 and $n\text{C}_4$.

The amount of gas components is controlled not only by gas migration, but also by the gas generation ability within the shale system. Generally, gas components with major differences in migration ability show strong gas fractionation, whereas gas components with minor differences in migration ability show poor gas fractionation [13,15,27]. For the accumulated gas, the retained gas and the generated gas in the YC23 Well, the gas fractionation of CH_4 and C_2H_6 was very significant (Figure 12c). However, the carbon isotopes of CH_4 and C_2H_6 showed a concentrated distribution, indicating poor gas fractionation (Figure 12d). For the heavy gases including propane, and n-butane, there was no gas fractionation (Figure 12e,f). This further proves that the difference in the values of $\delta^{13}\text{C}_2$ is not caused by gas migration, but is likely to be caused by the gas generation. Similarly, the differences in the content of heavy gases is not caused by gas migration, but by the gas generation.

Thus, it can be inferred that there are content differences among the gas compositions stored in different locations due to gas migration. For the gas components, CH_4 is easier to migrate than heavy hydrocarbon gases; N_2 is easier to migrate than CO_2 ; $\delta^{13}\text{C}_1$ is easier to migrate than other carbon isotopes; and lighter $\delta^{13}\text{C}_1$ is easier to migrate than heavier $\delta^{13}\text{C}_1$.

7. Conclusions

The average volume of desorbed gas in Chang-7 shale is $1.25 \text{ m}^3/\text{t}$. The Chang-7 shale gas is an oil-type gas of thermogenic origin, and the parent material of Chang-7 shale gas is mainly sapropel organic matter.

The Chang-7 shale gas in the YC23 Well can be sorted into three categories including generated gas, retained gas and accumulated gas.

For the YC23 Well, shale gas in different locations has unique components due to migration differences. The distribution of the gas components within the shale system is an effective indicator of gas migration.

Author Contributions: B.F. designed the project; B.F. wrote this paper and L.S. corrected it; B.F. performed the experiments; X.W., C.W., Y.L. and F.H. analyzed the data and drew the figures. All authors have read and agreed to the published version of the manuscript.

Funding: This study is supported by the Natural Science Foundation of Sinopec Key Laboratory of Shale Oil/Gas Exploration and Production Technology (33550000-21-ZC06130322).

Acknowledgments: We thank the Sinopec Key Laboratory of Shale Oil/Gas Exploration and Production Technology for providing funding for this project. We are grateful to the editors and reviewers for their constructive comments and suggestions.

Conflicts of Interest: The authors declare no conflict of interest.

References

1. Bertard, C.; Bruyert, B.; Gunther, J. Determination of desorbable gas concentration of coal (direct method). *Int. J. Rock Mech. Min. Sci. Geomech. Abstr.* **1970**, *7*, 43–65. [[CrossRef](#)]
2. Yee, D.; Seidle, J.P.; Hanson, W.B. Gas Sorption on Coal and Measurement of Gas Content. In *Hydrocarbons from Coal*; American Association of Petroleum Geologists: Tulsa, OK, USA, 1993; pp. 203–218. ISBN 978-1-6298-1104-8.
3. Han, H.; Li, D.; Ma, Y.; Cheng, L.; Zhong, N. The origin of marine shale gas in the northeastern Sichuan Basin, China: Implications from chemical composition and stable carbon isotope of desorbed gas. *Shiyou Xuebao/Acta Pet. Sin.* **2013**, *34*, 453–459.
4. Fan, B.J.; Wang, X.Z.; Shi, L. Gas desorption of low-maturity lacustrine shales, triassic yanchang formation, Ordos Basin, China. *Open Geosci.* **2018**, *10*, 688–698. [[CrossRef](#)]
5. Sun, Z.P.; Wang, Y.L.; Wei, Z.F.; Zhang, M.F.; Wang, G.; Wang, Z.X. Characteristics and origin of desorption gas of the Permian Shanxi Formation shale in the Ordos Basin, China. *Energy Explor. Exploit.* **2017**, *35*, 792–806. [[CrossRef](#)]
6. Stainforth, J.G. Practical kinetic modeling of petroleum generation and expulsion. *Mar. Pet. Geol.* **2009**, *26*, 552–572. [[CrossRef](#)]
7. Stewart, B.W.; Capo, R.C.; Kirby, C.S. Geochemistry of unconventional shale gas from formation to extraction: Petrogenesis, hydraulic fracturing, and environmental impacts. *Appl. Geochem.* **2015**, *60*, 1–2. [[CrossRef](#)]
8. Bruns, B.; Littke, R.; Gasparik, M.; van Wees, J.D.; Nelskamp, S. Thermal evolution and shale gas potential estimation of the Wealden and Posidonia Shale in NW-Germany and the Netherlands: A 3D basin modelling study. *Basin Res.* **2016**, *28*, 2–33. [[CrossRef](#)]
9. Charoensuppanimit, P.; Mohammad, S.A.; Gasem, K.A. Measurements and modeling of gas adsorption on shales. *Energy Fuels* **2016**, *30*, 2309–2319. [[CrossRef](#)]
10. Hu, Z.Q.; Du, W.; Sun, C.X.; Wu, J.; Zhu, T.; Zhao, J.H.; Yan, C.N. Evolution and migration of shale facies and their control on shale gas: A case study from the Wufeng-Longmaxi Formations in the Sichuan Basin and its surroundings. *Interpretation* **2018**, *6*, 57–70. [[CrossRef](#)]
11. Wang, X.Z. Characteristics of Chang 7 shale gas in the triassic Yanchang formation, Ordos basin, China. *Interpretation* **2017**, *5*, 31–39. [[CrossRef](#)]
12. Cui, J.W.; Zhu, R.K.; Luo, Z.; Li, S. Sedimentary and geochemical characteristics of the Triassic Chang 7 member shale in the southeastern Ordos Basin, Central China. *Pet. Sci.* **2019**, *16*, 285–297. [[CrossRef](#)]
13. Zhang, T.W.; Sun, X.; Ruppel, S.C. Hydrocarbon geochemistry and pore characterization of the Bakken Formation and implications for oil migration and oil saturation. In Proceedings of the 2013 Meeting of Mudrock Systems Research Laboratory, Pittsburgh, PA, USA, 19–22 May 2013; pp. 166–178.
14. Neal, R.O. Shale lamination and sedimentary processes. *Geol. Soc. Lond. Spec. Publ.* **1996**, *116*, 23–36. [[CrossRef](#)]
15. Fathi, E.; Akkutlu, I.Y. Matrix heterogeneity effects on gas transport and adsorption in coalbed and shale gas reservoirs. *Transp. Porous Media* **2009**, *80*, 281–304. [[CrossRef](#)]
16. McCarthy, J.F. Analytical models of the effective permeability of sand-shale reservoirs. *Geophys. J. Int.* **1991**, *105*, 513–527. [[CrossRef](#)]
17. Tao, H.; Pang, X.Q.; Shu, J.; Wang, Q.F.; Zheng, X.W.; Ding, X.G.; Zhao, Y.; Zhu, C.X.; Hui, L. Oil content evaluation of lacustrine organic-rich shale with strong heterogeneity: A case study of the middle permian lucaogou formation in jimusaer sag, junggar basin, NW China. *Fuel* **2018**, *221*, 196–205.
18. Fan, B.J.; Shi, L.; Li, Y.T.; Zhang, T.J.; Lv, L.; Tong, S.K. Lithologic heterogeneity of lacustrine shale and its geological significance for shale hydrocarbon—a case study of Zhangjiatan shale. *Open Geosci.* **2019**, *11*, 101–112. [[CrossRef](#)]
19. Li, H.; Tang, H.M.; Zheng, M.J. Micropore structural heterogeneity of siliceous shale reservoir of the Longmaxi formation in the southern Sichuan Basin, China. *Minerals* **2019**, *9*, 548. [[CrossRef](#)]
20. Fan, B.J. Effect of lithological heterogeneity on shale oil occurrence—A case study in Ansai oil field. *Arab. J. Geosci.* **2022**, *15*, 107.

21. Fan, B.J.; Shi, L. Deep-lacustrine shale heterogeneity and its impact on hydrocarbon generation, expulsion, and retention: A case study from the upper triassic Yanchang Formation, Ordos Basin, China. *Nat. Resour. Res.* **2019**, *28*, 241–257. [[CrossRef](#)]
22. Wang, Z.W.; Wang, J.; Fu, X.G.; Zhan, W.Z.; Armstrong-Altrin, J.S.; Yu, F.; Feng, X.L.; Song, C.Y.; Zeng, S.Q. Geochemistry of the Upper Triassic black mudstones in the Qiangtang Basin, Tibet: Implications for paleoenvironment, provenance, and tectonic setting. *J. Asian Earth Sci.* **2018**, *160*, 118–135. [[CrossRef](#)]
23. Fan, B.J. Characteristics and Origin of Organic Matter in Triassic Lacustrine Shale from Fuxian Oilfield. *Front. Earth Sci.* **2021**, *9*, 752954.
24. Bernard, B.; Brooks, J.M.; Sackett, W.M. A geochemical model for characterization of hydrocarbon gas sources in marine sediments. In Proceedings of the Offshore Technology Conference, Houston, TX, USA, 2 May 1977; pp. 435–438. [[CrossRef](#)]
25. Huang, Z.L.; Liu, G.H.; Li, T.J.; Li, Y.T.; Yin, Y.; Wang, L. Characterization and control of mesopore structural heterogeneity for low thermal maturity shale: A case study of Yanchang Formation Shale, Ordos Basin. *Energy Fuels* **2017**, *31*, 11569–11586. [[CrossRef](#)]
26. Zou, C.N.; Pan, S.Q.; Horsfield, B.; Yang, Z.; Hao, S.Y.; Liu, E.T.; Zhang, L.F. Oil retention and intrasource migration in the organic-rich lacustrine chang 7 shale of the upper triassic yanchang formation, ordos basin, central china. *AAPG Bull.* **2019**, *103*, 2627–2663. [[CrossRef](#)]
27. Wang, X.F.; Li, X.F.; Wang, X.Z.; Shi, B.G.; Luo, X.R.; Zhang, L.X.; Lei, Y.H.; Jiang, C.F.; Meng, Q. Carbon isotopic fractionation by desorption of shale gases. *Mar. Pet. Geol.* **2015**, *60*, 79–86. [[CrossRef](#)]
28. Wang, Q.; Fu, X.; Xu, Z. Development and application of stable carbon isotopes in natural gas and oil geochemistry. *Nat. Gas Geosci.* **2005**, *16*, 233–237, (In Chinese with English Abstract).
29. Song, Y.; Xu, Y.C. Origin and identification of natural gas. *Pet. Explor. Dev.* **2005**, *32*, 24–29.
30. Dai, J.X.; Gong, D.Y.; Ni, Y.Y.; Yu, C.; Wu, W. Genetic types of the alkane gases in giant gas fields with proven reserves over $1000 \times 108 \text{ m}^3$ in China. *Energy Explor. Exploit.* **2014**, *32*, 1–18. [[CrossRef](#)]
31. Jarvie, D.M.; Hill, R.J.; Ruble, T.E.; Pollastro, R.M. Unconventional shale-gas systems: The Mississippian Barnett Shale of north-central Texas as one model for thermogenic shale-gas assessment. *AAPG Bull.* **2007**, *91*, 475–499. [[CrossRef](#)]
32. Akihiko, O. Current understanding of hydrocarbon generation and migration in shale rocks. *J. Jpn. Assoc. Pet. Technol.* **2013**, *78*, 5–15.
33. Hammond, P.A. The relationship between methane migration and shale-gas well operations near Dimock, Pennsylvania, USA. *Hydrogeol. J.* **2015**, *24*, 503–519. [[CrossRef](#)]
34. Lin, S.H.; Zhi, Y.; Hou, L.H.; Xia, L.; Qun, L. Geostatistic recognition of genetically distinct shale facies in upper Triassic chang 7 section, the Ordos Basin, North China. *Mar. Pet. Geol.* **2019**, *102*, 176–186.
35. Clarkson, C.R.; Solano, N.; Bustin, R.M.; Bustin, A.M.M.; Chalmers, G.R.; He, L.; Melnichenko, Y.B.; Radliński, A.P.; Blach, T.P. Pore structure characterization of North American shale gas reservoirs using USANS/SANS, gas adsorption, and mercury intrusion. *Fuel* **2013**, *103*, 606–616. [[CrossRef](#)]
36. Du, X.D.; Gu, M.; Liu, Z.J.; Zhao, Y.; Sun, F.L.; Wu, T.F. Enhanced shale gas recovery by the injections of CO_2 , N_2 , and CO_2/N_2 mixture gases. *Energy Fuels* **2019**, *33*, 5091–5101. [[CrossRef](#)]
37. Dai, J.X.; Ni, Y.Y.; Gong, D.Y.; Feng, Z.Q.; Liu, D.; Peng, W.L.; Han, W.X. Geochemical characteristics of gases from the largest tight sand gas field (Sulige) and shale gas field (Fuling) in China. *Mar. Pet. Geol.* **2016**, *79*, 426–438. [[CrossRef](#)]
38. Li, W.B.; Lu, S.F.; Li, J.Q.; Zhang, P.F.; Wang, S.Y.; Feng, W.J.; Wei, Y.B. Carbon isotope fractionation during shale gas transport: Mechanism, characterization and significance. *Sci. China Earth Sci.* **2020**, *63*, 674–689. [[CrossRef](#)]
39. Li, J.L.; Zhang, T.S.; Li, Y.J.; Liang, X.; Wang, X.; Zhang, J.H.; Zhang, Z.; Shu, H.L.; Rao, D.Q. Geochemical characteristics and genetic mechanism of the high- N_2 shale gas reservoir in the Longmaxi Formation, Dianqianbei Area, China. *Pet. Sci.* **2020**, *17*, 939–953. [[CrossRef](#)]